CORE
Metadata, citation and similar papers at core.ac.uk
Provided by Repository of Faculty of Science, University of Zagreb

PHYSICAL REVIEW B **82**, 165205 (2010)

Beyond the effective temperature: The electron ensemble at high electric fields in disordered organics

I. Jurić,[1,*] I. Batistić,[2] and E. Tutiš[1,†]
[1]*Institute of Physics, Bijenička c. 46, HR-10000 Zagreb, Croatia*
[2]*Department of Physics, Faculty of Science, University of Zagreb, Bijenička c. 32, HR-10000 Zagreb, Croatia*
(Received 26 August 2010; published 29 October 2010)

Hopping between localized polaronic states, with a Gaussian distribution in energy, is regarded as the main mechanism of electric conduction in disordered organics. Several authors have recently suggested that the hopping electrons, subjected to an electric field, can be described as a homogeneous 'overheated' gas, with its "effective temperature" sufficient for a parametrization of the ensemble and the current. It is not clear how such a picture could be reconciled with the observed strongly oriented filamentization of the flow. We show, through extensive numeric simulations, that the picture is misleading as it can overestimate the electron mobility by orders of magnitude. The reason lies in deviations of the average site occupancies from the effective Boltzmann distribution. The ensemble can be described by a distribution function with two parameters—the effective temperature and the variance of the occupancy deviations. The two are connected by a simple universal relation. The spatial structure of the occupancy deviations is found to be connected to the current filaments and its neglect is recognized as the cause for the failure of mobility calculations based on the overheated gas concept. Thus we identify those aspects, lying beyond the overheated gas picture, that are of a fundamental importance to a proper understanding of the transport in disordered organics.

DOI: 10.1103/PhysRevB.82.165205 PACS number(s): 72.20.Ee, 72.20.Ht, 72.80.Le, 72.80.Ng

I. INTRODUCTION

Semiconducting organic materials have within last two decades progressed from an experimental curiosity to one of base components of consumer electronics.[1–3] They vary in structure from small-molecule glasses to spaghetti tangles of long conjugated polymer chains. It is established[4,5] that in these materials the conducting electrons and holes are localized on single molecules or segments of polymer chains. There is a pronounced disorder in their molecular energy levels with a Gaussian shaped electronic density of states (DOS).[4–8] The charge transport is realized through a thermally induced hopping between the localized states. It is characterized by a highly field-dependent mobility,[9] usually with the Pool-Frenkel behavior [$\mu \sim \exp(\text{const} \cdot \sqrt{F})$, where F is the electric field]. Significant efforts were devoted to explain the transport characteristic at high fields and a lot has been achieved. Namely, the existence of spatial correlations in the energy landscape was shown to be crucial to explain the mobility characteristic.[10–15] However, our understanding of the transport mechanism, particularly of the qualitative picture behind the numbers, is still not complete. Recently, the concept of an effective temperature has been evoked to assist in a formation of such a picture.[16,17]

The idea of an effective temperature comes from the observations that for a steady-state hopping transport in a disordered medium under influence of an external field, the ensemble of transporting carriers (electrons or holes) appears as if it was in a thermodynamic equilibrium. The distribution of carriers over energies is governed by a temperature that is higher than the real temperature of the environment (i.e., of the phonon bath assisting the hopping transport). This *effective* temperature is a function of the driving field strength and of the real environment temperature. From this observation stems a proposition that the transporting ensemble can really be described as, and replaced by, an equilibrium ensemble, and that the corresponding effective temperature can be used as the sole parameter determining the transport properties, such as the carrier mobility.

However, the picture of the transporting ensemble as an overheated, homogeneous "gas" of carriers thermalized at an elevated temperature, is at odds with the observations of current filaments in a steady-state flow.[15,18–20] The current flow is concentrated in a filamentary spatial structure possessing a strong directionality. The effect is particularly pronounced when the energy landscape is spatially correlated. How can it be that the transporting ensemble appears simultaneously describable by two fundamentally conflicting pictures? We explore this question in the present article. We investigate the observed heating of the transporting ensemble in a Gaussian disorder to determine to what extent the picture of an overheated carrier gas is valid, and whether it can reproduce relevant transport properties such as the mobility. We then show how the overheated gas picture connects to the filamentization of the flow.

The effective temperature phenomenon was first observed for an exponential-shaped density of states used in description of hoping transport in band tails of doped inorganic amorphous semiconductors.[21–24] There, the effective temperature could successfully parametrize the conductivity[21] and the time needed for relaxation to a steady state.[22] Recent works[16,17,25] have shown that the effective temperature also exists for a Gaussian-shaped density of states, in as much in that it can describe the distribution of carriers over site energies. In the first work,[16] Preezant and Tessler took an unusual approach of solving a master equation for the carrier distribution in the energy space. This approach is at best limited to a noncorrelated energy landscape, where it assumes the same effective environment for all sites. The second work by Jansson *et al.*[17] took a more common approach

 ©2010 The American Physical Society

of solving a master equation for the site occupancies in the real space but on a rather small grid of 20^3 sites. They found an effective temperature both in a noncorrelated and in a correlated energy landscape. In the noncorrelated case they used it to parametrize the mobility. In both works a finite density of carriers was considered, even though it can only be treated in a mean-field manner within a master equation approach. However, they found that the effective temperature does not depend on the carrier density, indicating that as far as the study of effective temperature is considered, a limit of low carrier density can be used. Both works utilized the Miller-Abrahams form of the hopping law. We have recently considered whether an effective temperature can describe the ensemble for a simpler case of a one-dimensional chain of noncorrelated energies.[25] We have found that it emerges in an approximate description of the carrier distribution over energies, and derived an analytical expression for it.

In this paper we solve a master equation in the real space to find the average carrier density in a stationary flow. We avoid the issue of errors inherent in mean-field approximations[26] by looking at the limit of low carrier density. Prior works[16,17] suggest that this should not change important ensemble properties (the effective temperature) but a low carrier density is also the actual regime in which many devices based on organic materials function (for example, density of one carrier per 10^6 molecules in organic light-emitting diodes[27]). Considering the stated importance of spatial correlations in disorder, we look at the correlated and the noncorrelated case in parallel. We start by expressing the state of the ensemble in terms of the average occupancy n_i of a site i with an energy E_i. Under conditions of a steady-state flow, we shall find it advantageous to re-express the heated ensemble in a new way. The ensemble thus re-expressed can be linked to spatial formations in the current flow.

The paper is arranged as follows: in Sec. II our method is presented—what we simulated and how the calculations were made. In Sec. III we present our findings regarding the effective temperature of the transporting ensemble and of how it relates to the mobility. In Sec. IV we take a look at the ensemble from another point of view. We find that it can be described with two parameters (one being the aforementioned effective temperature) and we find a universally valid relationship connecting the two. With insights gained in Sec. IV, we consider spatial correlations of variables in our redefined ensemble in Sec. V, and connect them with the known effect of the filamentization of the flow in a correlated disordered medium.[15]

II. METHOD

We model the energetically disordered medium in a familiar fashion,[10,12,15,17,19,20,28–31] as a regular rectangular grid of $L\times L\times L$ sites, each representing a molecule (or a segment of a conjugated polymer) with a spatially localized electron state (corresponding to the lowest unoccupied molecular orbital for electrons and the highest occupied molecular orbital for holes). The state at a site i, has its energy level E_i picked from the Gaussian density of states centered around $\langle E\rangle=0$, with standard variance σ_E,

$$g(E) = N(E,0,\sigma_E), \tag{1}$$

where $N(E,\langle E\rangle,\sigma_E)$ is the normal distribution in E, with mean $\langle E\rangle$ and variance σ_E,

$$N(E,\langle E\rangle,\sigma_E) \equiv \frac{1}{\sigma_E\sqrt{2\pi}}\exp\left[-\frac{(E-\langle E\rangle)^2}{2\sigma_E^2}\right]. \tag{2}$$

A spatial correlation among the energies is imposed by smoothing the initial energy landscape. The smoothing is achieved by averaging over $(2\times 3L_c+1)^3$ nearby sites with a Gaussian weight function of variance L_c. This produces a spatial correlation function for energies with a Gaussian profile. We choose a Gaussian smoothing mask over a flat mask[10] because the later introduces strong artificial kinks in spatial correlation functions. After the averaging procedure, the resulting energies are rescaled so that their variance remains the same as before the averaging process. The correlation so implemented differs from one created by a dipolar disorder,[11,12,14,32] which decays as $\sim r^{-1}$, in that it is of finite range. By considering a finite range correlation, we can study how properties of the transporting ensemble change with the correlation length. We consider in parallel the case of noncorrelated energies ($L_c=0$), and the cases of correlated energies with $L_c=1$ and $L_c=2$. Physically, an energy correlation of finite range is expected in conjugated polymers with strong intramolecular interactions,[15] and in molecular materials due to orientational and positional correlations,[10,33] and molecular polarizability.[32]

A charge carrier is allowed to hop through the grid under the influence of an external electric field F, applied along one of the grid axis, designated as x. The hopping probability (in unit time) from a site i to a site j can generally be expressed as a product of two factors, one depending on the distance r_{ij} between the sites, and the other on their energies E_i and E_j (modified by a superimposed external electric potential, $E_i \rightarrow E_i - Fq_e x_i$),

$$P_{i\rightarrow j} = \exp(-2\alpha r_{ij})\Omega(E_i,E_j). \tag{3}$$

The exponential dependence on the distance r_{ij} is determined by the electron wave-function attenuation rate α. The exact form of the energy-dependent factor $\Omega(E_i,E_j)$ depends on details of the physical system that is simulated but it should satisfy the microbalance principle,

$$\Omega(E_i,E_j) = \exp\left(\frac{E_i-E_j}{T_{real}}\right)\Omega(E_j,E_i), \tag{4}$$

where T_{real} is the environment temperature expressed in energy units. Previous articles[16,17] assumed an adiabatic form for $\Omega(E_i,E_j)$, known as the Miller-Abrahams[34] form,

$$\Omega_{MA}(E_i,E_j) = \omega_0\exp\left(\frac{E_i-E_j-|E_i-E_j|}{2T_{real}}\right), \tag{5}$$

where ω_0 is the base hopping frequency. However, there is strong evidence[10,14] that a diabatic, multiphonon, polaron transfer[35] is the real hopping mechanism in amorphous organics. In the limiting case of a large binding energy of a polaron to the lattice,[14] this mechanism leads to the so-called "symmetric" form for the hopping rate,

$$\Omega_{sym}(E_i,E_j) = \omega_0 \exp\left(\frac{E_i - E_j}{2T_{real}}\right). \quad (6)$$

In this paper, the symmetric form of the hopping law is used—as it is more befitting for a description of the electron transport in organics, except in part of Sec. III where the Miller-Abrahams form is used (and its usage noted explicitly) for a direct comparison with the results of previous papers. Note that, when it comes to calculating transport quantities, such as the current densities and the mobility, the specific choice of the hopping law was shown to make little difference.[12,15,28]

In the limit of small density n_i of carriers, the continuity equations for the currents $j_{i\to k}$, flowing from a site i to nearby sites k, become linear,

$$\frac{dn_i}{dt} = -\sum_k j_{i\to k} = \sum_k (n_k P_{k\to i} - n_i P_{i\to k}). \quad (7)$$

By equating dn_i/dt with zero, we obtain a set of linear equations for the average occupancies n_i of sites in the stationary (steady-state) flow. Periodic boundary conditions are applied to expand the simulated grid into an infinite bulk. The equations can be efficiently solved by available linear solvers (e.g., the PARDISO library[36–38]) for boxes of a medium size. The equations are solved for several realizations of the energy disorder, to improve the sampling and reduce statistical variations. Since the equations are linear, the solutions can be scaled by an arbitrary multiplicative factor, thus selecting a value for the average carrier density in the sample $\langle n_i \rangle$. This quantity factors out in the expressions for the mobility and the distribution functions. The occupancies are formed to the same value of $\langle n_i \rangle$ in each simulated box and all quantities calculated from them are averaged over disorder configurations.

For disordered amorphous organics with the separation between the molecules of several angstroms or greater, and the operating temperatures around the room temperature, the transport is expected to fall into the nearest-neighbor regime. We allow for the nearest- and the next-to-nearest neighbor hops in our calculation (i.e., hops along the grid by a distance of one lattice constant a_0 and along the face diagonals by a distance of $\sqrt{2}a_0$). Inclusion of more distant hops, with a reasonable value of α, was previously shown to be of no influence.[28,30,39,40] We have tested previously our master-equation algorithm, and our limitation to the next-to-nearest-neighbor regime, by comparing them with a multiparticle Monte Carlo approach in Ref. 28. Here we likewise compare our results with those of another, well-known, Monte Carlo simulation with a full variable range hopping implemented.[29] Figure 1. shows a next to perfect agreement of mobilities calculated by two completely different methods.

In this work we simulated a box of 60^3 sites,[41] larger boxes being prohibitively costly in memory and time to simulate.[42] Each calculation was made on ten configurations of the energy disorder. This allowed for a good estimation of errors inherent in sampling a finite system. The errors in the bulk properties (such as the effective temperature, the mobility, etc.) were generally negligible. Throughout the paper, we keep the lattice constant of the grid a_0 at 6 Å—a realistic value for materials composed of small organic molecules. The electron wave-function attenuation rate α is set to $5/a_0$. The field strength is expressed in megavolt per centimeter and the energies in electron volt. The variance σ_E of DOS is mostly kept at 0.06 eV and the environment temperature T_{real} at 300 K.

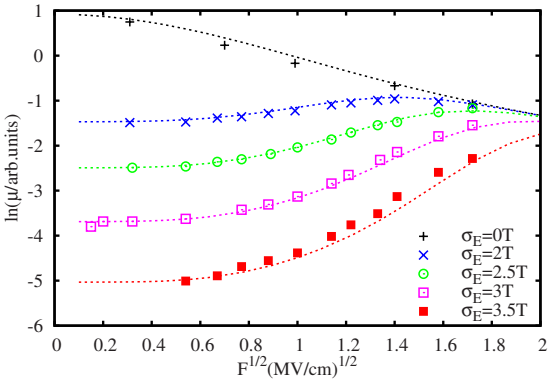

FIG. 1. (Color online) Logarithm of the mobility as a function of the square root of the electric field F. The points are results of a Monte Carlo calculation (Fig. 3 of Ref. 29) and the lines are solutions to our master equation. Both calculations use the Miller-Abrahams form of energy dependence [Eq. (5)], in a noncorrelated energy disorder with the variance σ_E expressed in terms of the environment temperature T_{real} set at 295 K. The lattice constant a_0 is 6 Å and the wave-function attenuation rate α is $5/a_0$. Our procedure for calculating the mobility is detailed in Sec. III.

III. EFFECTIVE TEMPERATURE AND THE MOBILITY

The first indication that the transporting ensemble can be described by an effective temperature comes from the distribution of carriers over energies,

$$O(E) = \sum_i n_i \delta(E - E_i) / \sum_i n_i. \quad (8)$$

When written as $O(E) = g(E)n(E)$, where

$$g(E) = \sum_i \delta(E - E_i) / \sum_i 1 \quad (9)$$

is the density of states, $n(E)$ will correspond to the average occupancy of sites with energy E,

$$n(E) = \frac{\sum_i n_i \delta(E - E_i)}{\langle n_i \rangle \sum_i \delta(E - E_i)}. \quad (10)$$

If an effective temperature exists, $n(E)$ will have an exponential form $n(E) = \exp(-E/T_{eff})$, for a low density of carriers, or a Fermi-Dirac form when finite densities are considered.[17] The effective temperature T_{eff} can then be identified from this form.

For a Gaussian density of states $g(E)$ and an exponential form of $n(E)$, $O(E)$ will also be a normal distribution. Specifically, for $g(E) = N(E, 0, \sigma_E)$,

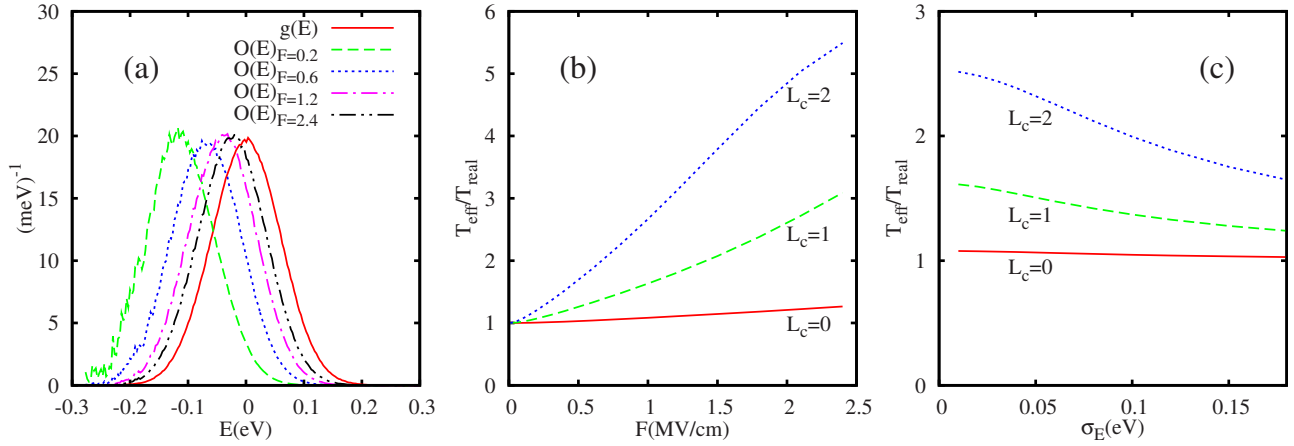

FIG. 2. (Color online) (a) The distribution of carriers over energies $O(E)$ for several field strengths and the density of states $g(E)$. The width of the DOS is σ_E=0.06 eV and the correlation length L_c=2. (b) The effective temperature dependence on the field strength for correlated and noncorrelated disorder, for σ_E=0.06 eV. (c) Dependence of the effective temperature on the width of the DOS σ_E, for F =0.8 MV/cm. In all three graphs the environment temperature is T_{real}=300 K.

$$O(E) = N\left(E, -\frac{\sigma_E^2}{T_{eff}}, \sigma_E\right). \tag{11}$$

As seen in Fig. 2(a), our numerical simulations show that this is indeed the case. The effective temperature can then be determined from the position of the shifted Gaussians in the figure. This method was used by Preezant and Tessler.[16]

Another way to obtain the effective temperature is by a direct least-squares fit of the expected form of $\ln[n(E)]$ to the set of pairs $(E_i, \ln n_i)$ for all sites. This method was used by Jansson *et al.*[17] It is not *a priori* clear that these two methods should yield the same value for the effective temperature. We tested them, and they do produce the same results. The reason why this is so will be elucidated in the following section. We use the second method when evaluating the effective temperature in our figures.

So how does this effective temperature change with the conditions in the system? The dependence of the effective temperature on the field strength is shown in Fig. 2(b). One can see that the transport in a correlated disorder is strikingly different than in a noncorrelated one. The carrier ensemble apparently heats up much more effectively at a same field strength F when the site energies are correlated. This is in agreement with the results of Jansson *et al.*[17] The field dependence of the effective temperature is superlinear. Both previous works claimed that T_{eff} does not depend on the strength of energy disorder σ_E. We find this to be the case only in a noncorrelated disorder [Fig. 2(c)]. T_{eff} diminishes with growing σ_E in a correlated disorder, although this effect is not very pronounced.

Previous works[16,17] claimed that, for a transport in a Gaussian density of states with a noncorrelated disorder, the effective temperature T_{eff} can be expressed as a function of the real environment temperature T_{real}, and of the field strength F in the form

$$T_{eff}^{\beta} = T_{real}^{\beta} + (\gamma e a_0 F)^{\beta} \tag{12}$$

with the temperatures expressed in energy units. This form was taken from Marianer and Shklovskii,[21] who used it to parametrize the effective temperature in systems with an exponential density of states. For the parameters β and γ, Preezant and Tessler found the values of β=2 and γ=0.37, while Jansson *et al.* found β=1.54 and γ=0.64. We tested the validity of the relation, both for the Miller-Abrahams form of the hopping law (which was used in these works), and for the symmetric form. As seen in Fig. 3, we find that the effective temperature *cannot be* expressed by Eq. (12). Although a decent fit to Eq. (12) can be made for small values of F and a fixed value of T_{real} (with the exponent β around 1.5), the value of the prefactor γ will vary with T_{real}. The results of Preezant and Tessler can be explained as artifacts of an effective medium approximation they used. The reason for discrepancy with the results of Jansson *et al.* is harder to pinpoint. It could be due to a small size of the grid they used in the simulation or perhaps due to an insufficient sampling of the configuration space or a limited parameter range they tested.

The observation that the distribution of carriers over energies $O(E)$ can be described by a single parameter—the effective temperature, led to the idea that the same single parameter might be enough to determine the main transport quantity—the field-dependent mobility. Thus, the field strength and the environment temperature would enter into an expression for the mobility through the effective temperature. Note that this is the point where the two pictures of the transporting ensemble, outlined in Sec. I, come most directly into conflict. If we can really express the mobility in terms of one parameter that is blind to spatial nuances, then the observed settling of the flow in filaments does not significantly influence the transport efficiency. Jansson *et al.* found this to be the case for a noncorrelated disorder with the mobility dependent on the effective temperature and the carrier concentration. Since in a noncorrelated disorder the filamentization of the flow is less pronounced, the parametrization of mobility in terms of the effective temperature might indeed be possible in that case. We proceed to check the validity of this result.

The mobility in our model can be expressed as the average over all sites of the field component of the current j_{xi},

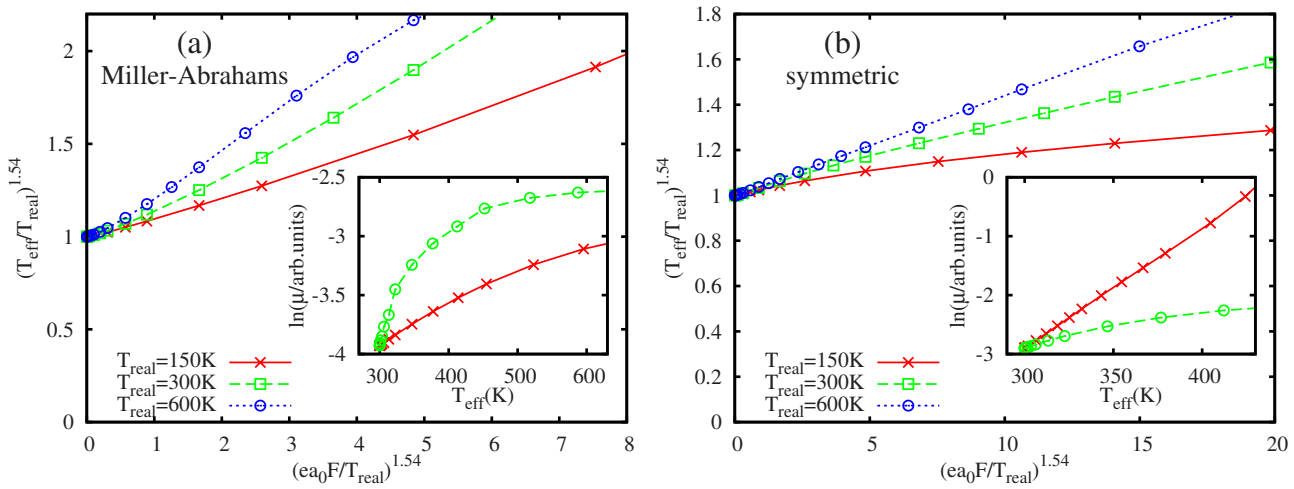

FIG. 3. (Color online) The main graphs: tests of Eq. (12) for (a) the Miller-Abrahams and (b) the symmetric form of the hopping law, with the parameter β set to 1.54, the value found by Jansson *et al.* (Ref. 17). Different lines have different, constant values of the environment temperature T_{real}, with the field strength F varied. If the Eq. (12) was valid, all lines would merge into one. The insets: logarithm of the mobility (in arbitrary units) as a function of the effective temperature of the ensemble. The full red line shows the mobility calculated for field strengths up to over 2 MV/cm in the Miller-Abrahams case and over 3.5 MV/cm in the symmetric case, at a constant environment temperature T_{real}=300 K. The dashed green line show the mobility calculated for a constant weak field F_0=0.01 MV/cm at higher environment temperatures (equal to the value of T_{eff} on the abscissa). In all graphs, the energy disorder is noncorrelated with σ_E =0.06 eV.

which is the total current flowing from a site i to its five (nearest- and next-to-nearest) neighbors situated downfield, divided by the field strength and the mean carrier density,

$$\mu = \langle j_{xi}\rangle / F\langle n_i\rangle. \tag{13}$$

The validity of T_{eff} parametrization of the mobility can be tested by comparing the mobility at some high field F and the room temperature, $\mu(F, T=300\ \text{K})$, with the mobility at a weak field F_0, and the environment temperature set to the corresponding value of high-field effective temperature, $\mu[F_0=0.01\ \text{MV/cm}, T_{eff}(F)]$. The two mobilities are presented in the insets of Fig. 3 for both types of the hopping law in a noncorrelated disorder. Opposite of the results of Jansson *et al.*, we find that the mobility *cannot be* parametrized by the effective temperature alone. The discrepancy between the two mobilities is even larger in the correlated disorder case (not pictured).

Why does the parametrization fail? The notion of an effective temperature comes from the observation that the transporting ensemble appears overheated. The assumption that accompanies this notion is that the transporting ensemble can indeed be effectively (for purposes of estimation of transport parameters) described as if overheated. This assumption can be directly tested by substituting the actual steady-state occupancies n_i with the corresponding equilibrium occupancies,

$$n_i \to n(E_i, T_{eff}) = \frac{\langle n_i\rangle}{A}\exp[-E_i/T_{eff}(F)], \tag{14}$$

where $A \equiv \Sigma_i \exp(-E_i/T_{eff})/\Sigma_i 1$ is the norm and T_{eff} changes with F as determined by the simulation. Clearly, the occupancies n_i cannot strictly follow a Boltzmann distribution, as the system is out of the equilibrium. The ansatz in Eq. (14), and the corresponding description of the ensemble as an overheated gas, can be considered appropriate if it can (1) reproduce relevant transport quantities (the mobility) well and (2) reproduce them better than if the occupancies n_i were replaced with $n(E_i, T_{real})$ (that is, if the effect of the electric field on the site occupancies was negligible).

If we calculate the mobility by replacing the currents j_{xi} in Eq. (13) with the values calculated from $n(E_i, T_{eff})$ or $n(E_i, T_{real})$ instead from the real occupancies n_i, the current continuity equations will not generally be satisfied at any site. But if the picture of a temperature-governed ensemble is valid, the average $\langle j_{xi}\rangle$ should still yield a good estimate of the mobility. There is a subtle but important difference between this substitution and the former simplistic parametrization of the mobility. While the occupancies are assumed in equilibrium at T_{eff}, the currents are calculated with the hopping rates determined by the real field strength and the environment temperature. The test is essentially of whether the distributions in Fig. 2(a) really show overheated equilibrium ensembles.

In Fig. 4 we compare the results for the mobility calculated from the $n(E_i, T_{eff})$ ansatz and the $n(E_i, T_{real})$ ansatz with the real values. It turns out that neither ansatz is valid and that the assumption of an equilibrium ensemble at T_{eff} yields even worse results than assuming that the carrier distribution is unaffected by the field. The discrepancy is significant even for a low disorder strength (σ_E=0.06 eV), and becomes huge, overestimating the mobility by orders of magnitude, for a stronger disorder (σ_E=0.12 eV). The difference between the mobility estimates increases with σ_E because the two exponential distributions in the ansatz differ more across several σ_E when that σ_E is larger compared to T_{eff} and T_{real}. The discrepancy is particularly pronounced in the correlated disorder case at low fields, where the ansatz-

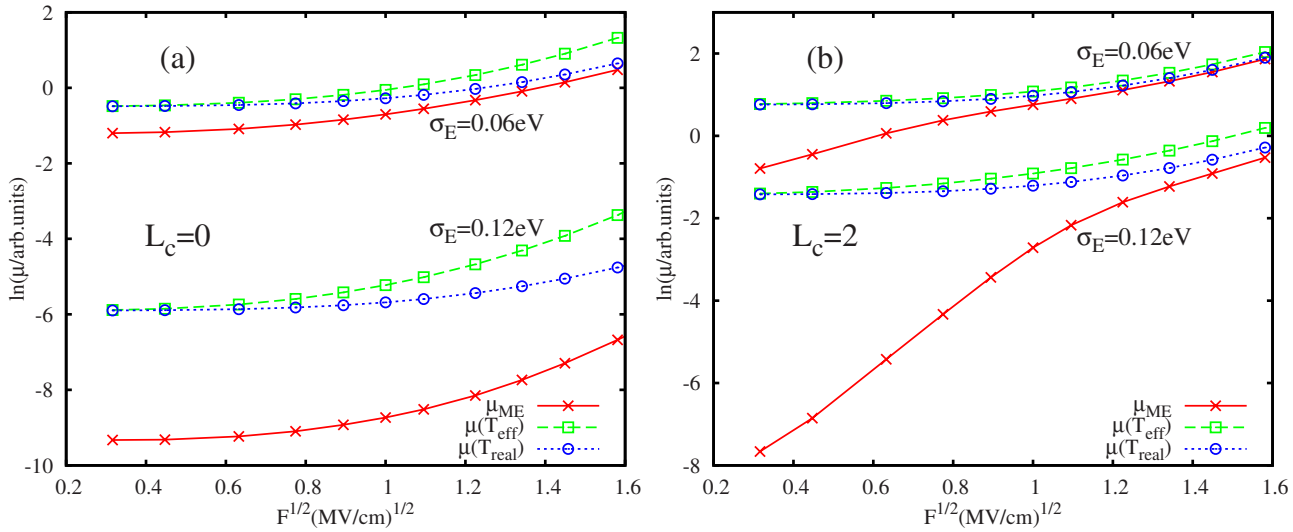

FIG. 4. (Color online) Logarithm of the mobility as a function of the square root of the field strength. (a) presents the noncorrelated disorder case and (b) the correlated case with L_c=2. The full red line is the real mobility obtained by solving the master equation. The green dashed line is the mobility calculated from the ansatz in Eq. (14). The blue doted line is mobility calculated from the same ansatz but with T_{eff} replaced by T_{real}=300 K. The upper set of lines is for σ_E=0.06 eV and the lower set for σ_E=0.12 eV. The lower set was additionally pushed downwards by 2, to make the sets clearly distinguishable.

based mobilities also fail to recreate a Pool-Frenkel type of field dependence. The fact that the mobility is overestimated even at low fields, when the occupancies n_i deviate little from the equilibrium ones, indicates that the key features of the transporting ensemble are glossed over by an equilibrium ansatz at any temperature. The picture of the ensemble as a gas of overheated carriers is essentially invalid.

IV. REPARAMETRIZATION OF THE ENSEMBLE

Since the substitution of the average occupancies n_i in a steady-state flow with the Boltzmann distribution $\exp(-E_i/T_{eff})$ fails to account for the mobility, a more detailed inspection of the ensemble is needed to gain a proper understanding of the transport. We consider the actual distribution of the occupancies n_i over the energies E_i of the sites, by looking at the distribution function $G(E,\ln n)$ of the grid sites over their $(E,\ln n)$ values in a two-parameter histogram. The distribution is appropriately scaled with the density of states $g(E)$,

$$G(E,\ln n) = \frac{\sum_i \delta(E-E_i)\,\delta(\ln n - \ln n_i)}{\sum_i \delta(E-E_i)}. \tag{15}$$

For an equilibrium ensemble at some temperature T, $G(E,\ln n)$ will be zero except on a line given by

$$\ln n = -E/T + C \tag{16}$$

with $C \equiv \langle \ln n_i \rangle$. In a transporting ensemble that appears to follow some effective temperature, deviations from such a perfect distribution are expected. Histogram in Fig. 5 shows the actual profile of the function $G(E,\ln n)$. The main features of $G(E,\ln n)$ visible in the histogram are present for all choices of the parameter values in the tested range. For any specific energy E, $G(E,\ln n)$ is a bell-shaped distribution in $\ln n$, with the mean given by Eq. (16). The width of the this distribution along the $\ln n$ axis does not depend on the energy E. Labeling this width as σ_δ, we can describe $G(E,\ln n)$ by two parameters, T_{eff} and σ_δ,

$$G(E,\ln n) = N(\ln n, -E/T_{eff} + C, \sigma_\delta). \tag{17}$$

The fact that the shape and the width of $G(E,\ln n)$ along the $\ln n$ axis does not change with E, is important. It ensures that the distribution of carriers over energies $O(E)$ will indeed be a shifted Gaussian, and consequently that the trans-

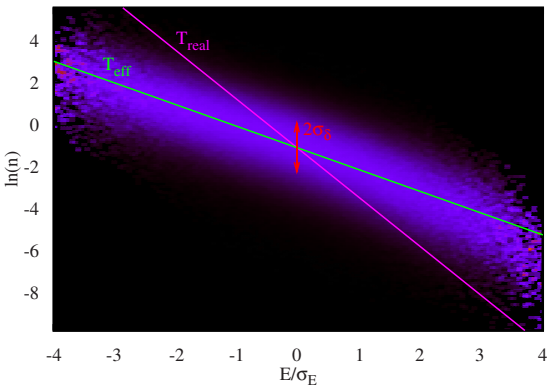

FIG. 5. (Color online) Histogram of the distribution function $G(E,\ln n)$ (purple) for σ_E=0.06 eV, F=0.8 MV/cm, and L_c=2. The green line (marked T_{eff}) corresponds to an equilibrium distribution given by Eq. (16) with $T=T_{eff}$. The magenta line (marked T_{real}) corresponds to $T=T_{real}$. The red arrows show the variance of the deviations from the equilibrium distribution at T_{eff}. The scattering visible at the edges is due to a poor statistic for sites whose energy is more than $3\sigma_E$ distant from the mean.

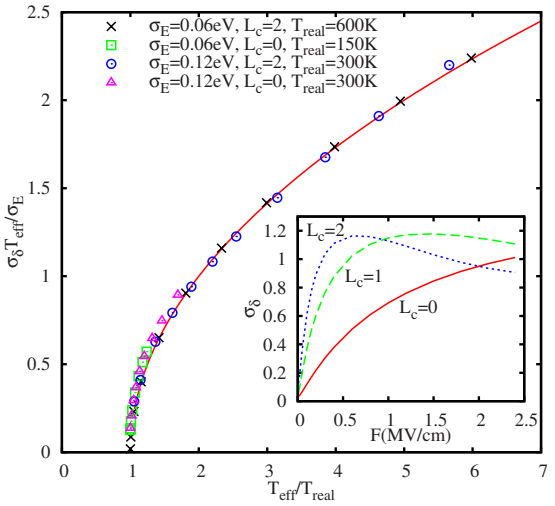

FIG. 6. (Color online) Agreement of σ_δ and T_{eff} with the relation in Eq. (18) (the red line) for several choices of parameter values. The inset shows dependence of the variance σ_δ on the field strength F for the three correlation lengths with σ_E=0.06 eV and T_{real}=300 K.

porting ensemble will appear to resemble an overheated gas. It further guarantees the equivalence of the effective temperature taken from the least-squares fit to the ensemble and the one read from the position of the $O(E)$ maximum. These conclusions can be reached through a simple straightforward calculation, outlined in the Appendix.

How does σ_δ depend on the field strength? The inset in Fig. 6 shows it growing with the field at first, reaching a maximum and later attenuating. The behavior may seem peculiar but it turns out there is a simple relation between $T_{eff}(F)$ and $\sigma_\delta(F)$. The main graph in Fig. 6 shows that σ_δ depends on the corresponding value of T_{eff} in a universal manner,

$$\sigma_\delta = \frac{\sigma_E}{T_{eff}} \sqrt{\frac{T_{eff} - T_{real}}{T_{real}}}. \tag{18}$$

This relation is valid both in a correlated and a noncorrelated disorder, over all tested fields F, disorder strengths σ_E, correlation lengths L_c, and environment temperatures T_{real}.

The distribution width σ_δ represents the deviation of the real transporting ensemble from the idealized ensemble in equilibrium at the same effective temperature. In the equilibrium, $\ln n_i$ would vary across the sites by $\sim \sigma_E / T_{eff}$. However, at any site we can expect $\ln n_i$ of the real transporting ensemble to deviate from this thermalized value by σ_δ. Thus the ratio of the two, $\sigma_\delta T_{eff}/\sigma_E = \sqrt{(T_{eff} - T_{real})/T_{real}}$ is a good measure of the "thermalization" of the transporting ensemble. However, since T_{eff} fails to reproduce the mobility at higher disorder strengths even when the ratio $\sigma_\delta T_{eff}/\sigma_E$ is small, it follows that the deviation of n_i values from $n(E_i, T_{eff})$ is important even when minute.

We now focus on this local deviation. It is advantageous to change our way of describing the ensemble [as the set of all $(E_i, \ln n_i)$ points], by replacing the average occupancy n_i with a new variable δ_i representing a logarithmic deviation at a site i from the expected occupancy given by the Boltzmann distribution $n(E_i, T_{eff})$,

$$\delta_i \equiv \ln n_i - (-E_i/T_{eff} + C). \tag{19}$$

The δ_i can be viewed as a logarithmically measured "overoccupancy" of a specific site i, with respect to other sites "on average" thermalized at T_{eff}. σ_δ is then the standard variance of δ_i. The distribution function $G(E, \ln n)$ becomes independent of the energy (and of the effective temperature) when restated in the new variables,

$$G(E, \delta) = N(\delta, 0, \sigma_\delta). \tag{20}$$

The spatial structure of the overoccupancies δ_i will be shown related to the current flow.

V. ENSEMBLE AND THE FILAMENTIZATION OF THE FLOW

It is known that the transport in a medium with a correlated disorder exhibits filamentization,[15] streams (filaments) form that carry majority of the current. These filaments are expected to form in the "ravines" or the "canyons" in the energy landscape, areas of lower-than-average energies. We show here that this filamentization can be seen in the current-current spatial correlations and the ravine preference in the current-energy correlations. We further show that a similar correlation pattern is present in the spatial correlations of the overoccupancies δ_i. The correlations are defined in the standard manner: the average (over all sites i and disorder configurations) of the product of two functions A and B at different positions i and $i+r$, separated by a distance r, corrected for their mean values, and scaled with their standard variances σ_A and σ_B,

$$C_{AB}(r) = \frac{\langle A_i B_{i+r} \rangle - \langle A_i \rangle \langle B_i \rangle}{\sigma_A \sigma_B}. \tag{21}$$

The correlations are viewed separately in the direction of the field and perpendicular to it, and correspondingly marked by the superscripts $\parallel$ and $\perp$. All correlations in the following figures are calculated for σ_E=0.06 eV and T_{real}=300 K.

When we refer to the current correlations we mean specifically the field-direction component of the current, j_x. The current-current spatial correlations for a correlated and a noncorrelated disorder are shown in the upper part of Fig. 7. In a noncorrelated disorder, the correlation $C_{jj}(r)$ falls off to zero (that is, to the background noise value) very fast. The falloff is a bit slower in the field direction than perpendicular to it. When the disorder is correlated, the current-current correlation will extend over the correlation length L_c perpendicular to the field, while in the field direction it will become long range[43] compared to L_c, lasting well over the simulated box size. This is a signature of the filament formation. The rate of the correlation falloff in the field direction corresponds to straightness of the meandering streams which straighten as the field gets stronger while the correlation profile perpendicular to the field essentially sketches the filament thickness.

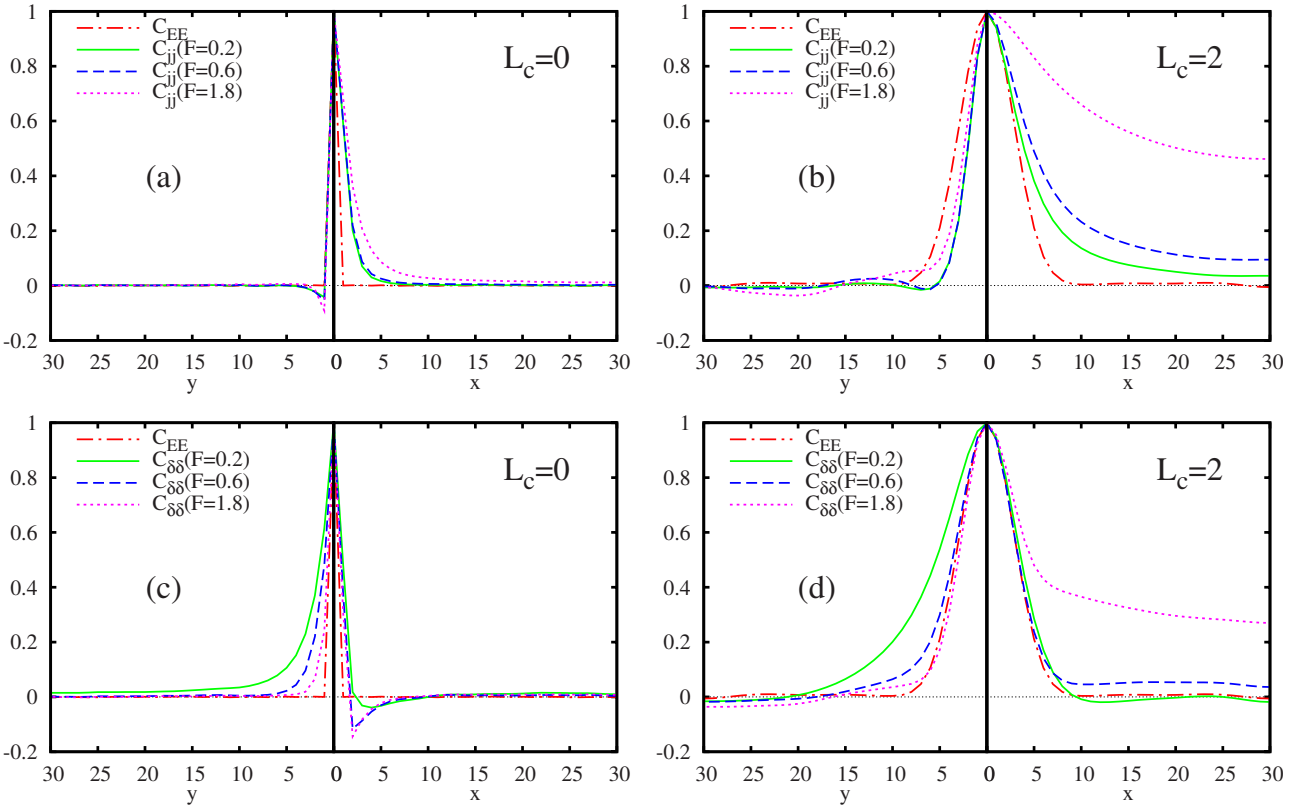

FIG. 7. (Color online) [(a) and (b)] The current-current autocorrelation $C_{jj}(r)$ and [(c) and (d)] the overoccupancy-overoccupancy autocorrelation $C_{\delta\delta}(r)$ for several field strengths. The figures on the left [(a) and (c)] are for a noncorrelated disorder and those on the right [(b) and (d)] are for a correlated disorder with $L_c=2$. In each graph, the correlation in a direction perpendicular to the field is pictured left of the ordinate axis, and the correlation in the direction of the field is pictured right of the axis. The red, dashed-dotted line is the autocorrelation profile of the site energies $C_{EE}(r)$.

Note should be taken of the omnipresent size effect, as 60 sites are too few to fully encompass the filamentary structures forming in the field direction. This is doubly inconvenient as the periodic boundary conditions will influence the geometry of such structures—filaments need to exit the simulated box where they entered. They are likely to be additionally strengthened and straightened due to this. Lack of such long-range correlations perpendicular to the field opens a possibility of simulating an elongated box of the same total number of sites, e.g., $240\times30\times30$. This solution neither is perfect as it constrains the lateral flow, i.e., meandering of the filaments. Still, the long-range correlations in the field direction are present in that case also, and the results do corroborate our findings and conclusions presented further on.

Consider now the analogous spatial autocorrelations of the overoccupancy δ_i, shown in the lower part of Fig. 7. In the correlated disorder case, the overoccupancy autocorrelation $C_{\delta\delta}(r)$ has a similar form to the current autocorrelation $C_{jj}(r)$, with the same type of filamentary profile noticeable. There is a long-range correlation in the field direction indicating a redistribution of the carriers into highly populated streams and a lowly populated background. The correlation perpendicular to the field, $C^{\perp}_{\delta\delta}(r)$, shows the filaments narrowing at higher fields. In a noncorrelated disorder there are no such long-range formations. There is a puzzling similarity and difference between the current and the overoccupancy autocorrelations in a noncorrelated disorder. The overoccupancy correlation in the field direction, $C^{\parallel}_{\delta\delta}$, mimics the current correlation perpendicular to it, $C^{\perp}_{jj}$. Both exhibit a short-range anticorrelation, likely connected to a small-scale redistribution of the carriers required to satisfy the current continuity relations at every site. The presence of this short-range anticorrelation is enough to cause the former mobility calculation based on the equilibrium occupancy ansatz to fail even for a noncorrelated disorder. In a similar manner, $C^{\perp}_{\delta\delta}$ appears to mimic $C^{\parallel}_{jj}$ but there is an important difference. The current autocorrelation strengthens with the field as the streams form even in a noncorrelated disorder. In contrast, the overoccupancy autocorrelation weakens at higher fields as the carriers spend less time wondering perpendicular to the field.

The current-energy correlations $C_{jE}(r)$ in the upper part of Fig. 8 show that the current at some site is generally anticorrelated with the energy of the site, demonstrating the ravine preference. It is also anticorrelated with the energies of the sites upstream (i.e., behind in the field direction). This is the filament's "memory," the streams are split or rerouted by high-energy sites, which act as barriers to the flow. Once a barrier is passed, it takes a substantial distance for a new stream to form after the barrier. This effect is present both in a noncorrelated and in a correlated disorder, but is signifi-

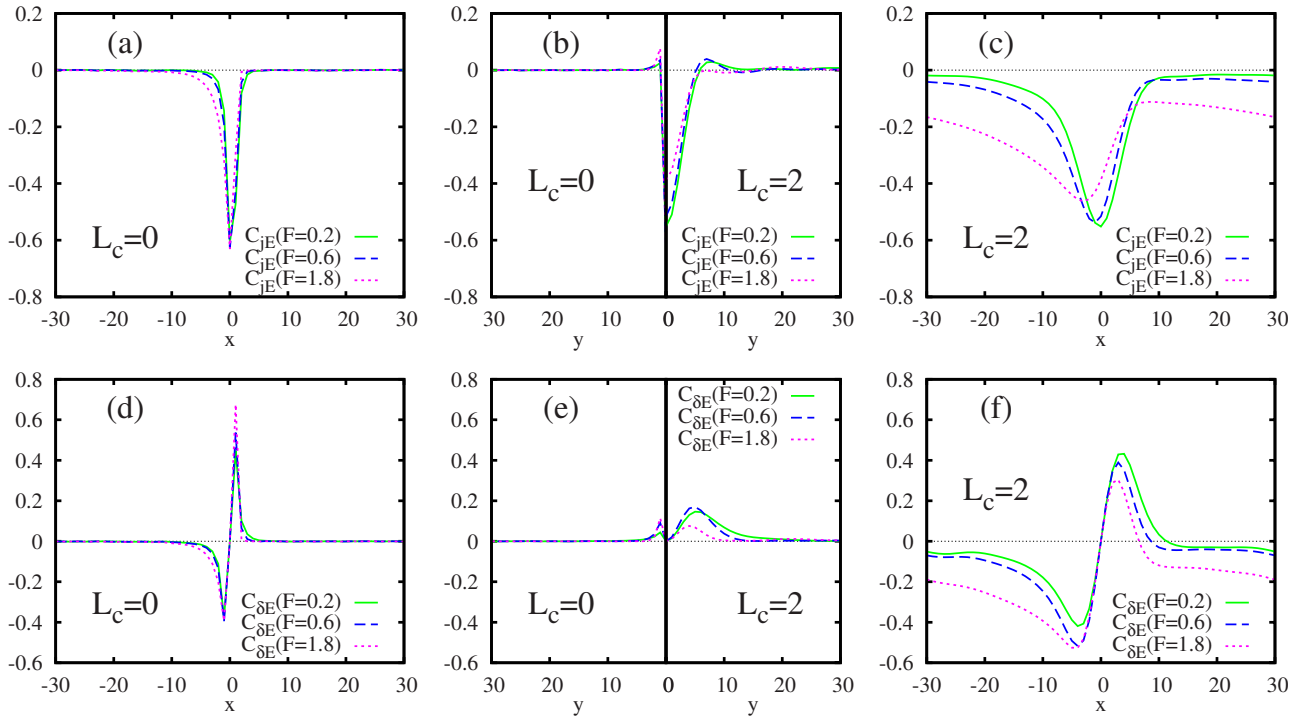

FIG. 8. (Color online) [(a)–(c)] The current-energy correlation $C_{jE}(r)$ and [(d)–(f)] the overoccupancy-energy correlation $C_{\delta E}(r)$ for several field strengths. (a) and (d) The correlations in the field direction for a noncorrelated disorder. (c) and (f) The correlations in the field direction for a correlated disorder with $L_c=2$. (b) and (e) The correlations in a direction perpendicular to the field for a noncorrelated disorder (left of the ordinate axis) and a correlated disorder (right of the ordinate axis).

cantly more pronounced, and of longer range in the correlated disorder case. Perpendicular to the field, the current-energy anticorrelation reaches only as far as the energies themselves are correlated. The strength of the on-site ($r=0$) anticorrelation diminishes as the field strength grows—the streams are less constrained and less affected by obstacles at stronger fields. However the rate of the correlation falloff in the upstream direction also diminishes, showing again that the field straightens the filaments, and once rerouted they will tend to stay thus.

The overoccupancy-energy spatial correlation $C_{\delta E}(r)$ in the lower part of Fig. 8 shows a slightly different pattern than the current-energy correlation. First thing easily noticeable is that the on-site correlation is exactly zero. It is easy to show that this is a consequence of the definition of δ_i [Eq. (19)], as the distribution function $G(E,\delta)$ shows no energy preference [Eq. (20)]. Since δ_i is independent of E_i, the influence of other sites (the surrounding energy landscape) can be clearly seen in the correlation $C_{\delta E}(r)$. Again, there is a clear difference between a correlated and a noncorrelated disorder. In a correlated disorder, there is a long-range anticorrelation present in the field direction, both upstream and downstream. This represents a general overoccupancy of the "canyons" in the energy landscape—those oriented in the field direction. The correlation $C^{\parallel}_{\delta E}(r)$ also features a short-range "kink" formation showing that an overoccupancy and an underoccupancy is present directly before and after nearby energy barriers. The maximum and the minimum of this short-range rearrangement of site occupancies are situated at the endreach of the energy correlation (a few L_c). Perpendicular to the field a subtle correlation is present at the same distance. Since the on-site correlation $C_{\delta E}(r=0)$ is zero, it will be faint perpendicular to the field as far as the energies themselves are correlated. The subtle positive correlation at that distance essentially sketches the "walls of the canyons," an overoccupancy is slightly more likely at a site if the energies in the neighboring area (within few L_c) are below average. In a noncorrelated disorder there are no long-range phenomena, but the short-range kink remains, again foiling the ansatz-based mobility calculation.

In summary, the matching profiles of the current and the overoccupancy correlations in the correlated case, and their similarities and differences in the noncorrelated case, demonstrate that the deviations from the T_{eff}, equilibrium distribution are connected with the small-scale redistribution of the flow (the kink in $C_{\delta E}$ and the anticorrelation in $C^{\parallel}_{\delta\delta}$), and, in a correlated disorder, with the formation of the filaments. There is a stark difference between drift transport regimes in a correlated and a noncorrelated disorder. Aside the obvious presence of the filamentization in the correlated disorder case, the spatial structure of the overoccupancies follows the structure of the current flow in the correlated but not in the noncorrelated case. This can be confirmed directly by looking at the on-site correlation between the overoccupancy and the current $C_{\delta j}(r=0)$ shown in Fig. 9. While $C_{\delta j}(r=0)$ grows quickly to a high value as the field increases in a correlated disorder, it remains negligible (and even negative) in the entire tested field range when $L_c=0$.

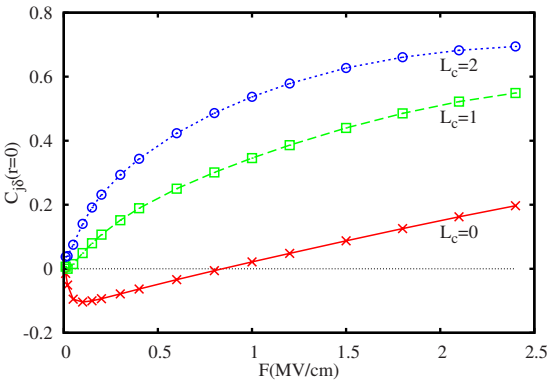

FIG. 9. (Color online) The on-site correlation between the overoccupancy and the current, $C_{\delta j}(r=0)$, as a function of the field strength F, for the three energy correlation lengths L_c.

VI. CONCLUSIONS

We have verified the existence of an elevated effective temperature as a property of the transporting ensemble in a Gaussian disorder and confirmed it to be is substantially higher when the disorder is correlated. However, we found it insufficient for a proper description of the transport. The picture of the carriers in a steady flow as essentially an overheated gas is wrong, as it cannot adequately explain the mobility. The deviations from a Boltzmann-type distribution hold a key ingredient for a proper understanding of the transport. The average variance of these overoccupancies σ_δ is directly connected to the effective temperature T_{eff} by a universally valid relation [Eq. (18)]. The distribution of occupancies over energies can be described by these two parameters [Eq. (17)]. We connect the overoccupancies with the flow structure, the filamentization of the current in a correlated disorder and the short-scale rearrangements of the flow in a noncorrelated and a correlated disorder. Thus fundamentally important information about the transport are found away from an effective temperature: in the spatial structure of the nonthermalized aspect of the ensemble, the overoccupancies. What is still lacking is a fruitful, quantitative model connecting the statistical ensemble properties (the effective temperature and the spatial structure of the overoccupancies) with the current filamentization and the bulk averaged properties such as the mobility. Development of such a model should be the aim of future efforts.

ACKNOWLEDGMENTS

The work presented in this paper was supported by the Croatian Ministry of Science, Education and Sports, under Grant No. 035-0352826-2847, and also by the Unity through Knowledge Fund, under Grant No. 65/10.

APPENDIX: CONNECTION BETWEEN THE SHAPE OF $G(E,\ln n)$ AND $O(E)$

Here we show what conditions the distribution function $G(E,\ln n)$, defined by Eq. (15), has to fulfill so that the distribution of carriers over energies $O(E)$ [Eq. (8)] would be a shifted Gaussian [Eq. (11)].

$O(E)$ can be expressed through $G(E,\ln n)$ and the density of states $g(E)$ [Eq. (9)] as

$$O(E) = \frac{1}{\langle n_i \rangle} \int \exp(\ln n) G(E,\ln n) g(E) d(\ln n). \quad \text{(A1)}$$

After switching to integration over the overoccupancy δ, defined by Eq. (19), we get

$$O(E) = \frac{1}{\langle n_i \rangle} g(E) \exp\left(-\frac{E}{T_{eff}} + C\right) \int \exp(\delta) G(E,\delta) d\delta. \quad \text{(A2)}$$

Equating this with Eq. (11) leads to

$$\int \exp(\delta) G(E,\delta) d\delta = \text{const}, \quad \text{(A3)}$$

i.e., the distribution $G(E,\delta)$ cannot be a function of the energy: $G(E,\delta)=f(\delta)$.

In other words, for the distribution of carriers over energies $O(E)$ to be a Gaussian, and consequently for the transporting ensemble to appear as if in equilibrium at some temperature T_{eff}, the shape and the width of the profile of $G(E,\ln n)$ along the $\ln n$ axis must not change with E while its center follows the Boltzmann line: $-E/T_{eff}+C$.

*ijuric@ifs.hr
†edo@ifs.hr

[1] S. R. Forrest, Nature (London) **428**, 911 (2004).
[2] T. W. Kelley, P. F. Baude, C. Gerlach, D. E. Ender, D. Muyres, M. A. Haase, D. E. Vogel, and S. D. Theiss, Chem. Mater. **16**, 4413 (2004).
[3] G. Malliaras and R. Friend, Phys. Today **58** (5), 53 (2005).
[4] S. Baranovski, *Charge Transport in Disordered Solids with Applications in Electronics* (Wiley, New York, 2006).
[5] N. Tessler, Y. Preezant, N. Rappaport, and Y. Roichman, Adv. Mater. **21**, 2741 (2009).
[6] A. J. Campbell, D. D. C. Bradley, and D. G. Lidzey, J. Appl. Phys. **82**, 6326 (1997).
[7] I. G. Hill, A. Kahn, J. Cornil, D. A. dos Santos, and J. L. Brédas, Chem. Phys. Lett. **317**, 444 (2000).
[8] N. Tessler and Y. Roichman, Org. Electron. **6**, 200 (2005).
[9] In this paper the mobility always refers to the electronic mobility measured in a steady-state flow. This is the relevant quantity when describing the functioning of organic electronic devices, all of which work in dc mode. It can differ from the so-called time-dependent mobility that is obtained in time-of-flight measurements on very thin samples (Refs. 44 and 45).
[10] Yu. N. Gartstein and E. M. Conwell, Chem. Phys. Lett. **245**, 351 (1995).

[11] D. H. Dunlap, P. E. Parris, and V. M. Kenkre, Phys. Rev. Lett. **77**, 542 (1996).
[12] S. V. Novikov, D. H. Dunlap, V. M. Kenkre, P. E. Parris, and A. V. Vannikov, Phys. Rev. Lett. **81**, 4472 (1998).
[13] P. E. Parris, D. H. Dunlap, and V. M. Kenkre, Phys. Status Solidi B **218**, 47 (2000).
[14] P. E. Parris, V. M. Kenkre, and D. H. Dunlap, Phys. Rev. Lett. **87**, 126601 (2001).
[15] Z. G. Yu, D. L. Smith, A. Saxena, R. L. Martin, and A. R. Bishop, Phys. Rev. B **63**, 085202 (2001).
[16] Y. Preezant and N. Tessler, Phys. Rev. B **74**, 235202 (2006).
[17] F. Jansson, S. D. Baranovskii, F. Gebhard, and R. Österbacka, Phys. Rev. B **77**, 195211 (2008).
[18] M. Cölle, M. Büchel, and D. M. de Leeuw, Org. Electron. **7**, 305 (2006).
[19] E. Tutiš, I. Batistić, and D. Berner, Phys. Rev. B **70**, 161202 (2004).
[20] E. Tutiš and I. Batistić, Fiz. A **14**, 167 (2005).
[21] S. Marianer and B. I. Shklovskii, Phys. Rev. B **46**, 13100 (1992).
[22] S. D. Baranovskii, B. Cleve, R. Hess, and P. Thomas, J. Non-Cryst. Solids **164-166**, 437 (1993).
[23] B. Cleve, B. Hartenstein, S. D. Baranovskii, M. Scheidler, P. Thomas, and H. Baessler, Phys. Rev. B **51**, 16705 (1995).
[24] P. Thomas and S. D. Baranovskii, J. Non-Cryst. Solids **164-166**, 431 (1993).
[25] E. Tutiš, I. Jurić, and I. Batistić, Croat. Chem. Acta **83**, 87 (2010).
[26] And also of the Coulomb interaction between the carriers, which is completely untractable in a master-equation approach (Ref. 31).
[27] E. Tutiš, D. Berner, and L. Zuppiroli, J. Appl. Phys. **93**, 4594 (2003).
[28] H. Houili, E. Tutiš, I. Batistić, and L. Zuppiroli, J. Appl. Phys. **100**, 033702 (2006).
[29] H. Bässler, Phys. Status Solidi B **175**, 15 (1993).
[30] W. F. Pasveer, J. Cottaar, C. Tanase, R. Coehoorn, P. A. Bobbert, P. W. M. Blom, D. M. de Leeuw, and M. A. J. Michels, Phys. Rev. Lett. **94**, 206601 (2005).
[31] S. V. Novikov, Phys. Status Solidi C **5**, 740 (2008).
[32] M. N. Bussac, J. D. Picon, and L. Zuppiroli, Europhys. Lett. **66**, 392 (2004).
[33] L. B. Schein, Philos. Mag. B **65**, 795 (1992).
[34] A. Miller and E. Abrahams, Phys. Rev. **120**, 745 (1960).
[35] D. Emin, Adv. Phys. **24**, 305 (1975).
[36] G. Karypis and V. Kumar, SIAM J. Sci. Comput. (USA) **20**, 359 (1998).
[37] O. Schenk and K. Gärtner, FGCS, Future Gener. Comput. Syst. **20**, 475 (2004).
[38] O. Schenk and K. Gärtner, Electron. Trans. Numer. Anal. **23**, 158 (2006).
[39] U. Wolf, V. I. Arkhipov, and H. Bässler, Phys. Rev. B **59**, 7507 (1999).
[40] R. Coehoorn, W. F. Pasveer, P. A. Bobbert, and M. A. J. Michels, Phys. Rev. B **72**, 155206 (2005).
[41] Other sizes, as the one mentioned in Sec. V, were also used.
[42] An iterative method of solving the equations may permit a simulation of substantially larger boxes (Ref. 15). We prefer a direct solver (PARDISO) here, as it is more accurate at low densities, compared to iterative methods.
[43] When we refer to the correlations as long-range in this paper, we mean that they are substantially longer (by an order of magnitude or more) than the only length scale present in the system, which is L_c. It is expected though that in an infinite bulk, the correlations would fall off to zero eventually.
[44] P. W. M. Blom and M. C. J. M. Vissenberg, Phys. Rev. Lett. **80**, 3819 (1998).
[45] Y. A. Berlin, L. D. A. Siebbeles, and A. A. Zharikov, Chem. Phys. Lett. **305**, 123 (1999).